

***Ab Initio* Structure Determination of Icosahedral Zn-Mg-Ho Quasicrystals by Density Modification Method**

Hiroyuki Takakura,^{1,2,*} Masaaki Shiono,³ Taku J. Sato,^{1,2} Akiji Yamamoto,⁴ and An Pang Tsai^{1,2}

¹*National Research Institute for Metals, Tsukuba 305, Japan*

²*CREST, Japan Science and Technology Corporation, Kawaguchi, Saitama, Japan*

³*Department of Physics, Faculty of Science, Kyushu University, Fukuoka 812, Japan*

⁴*National Institute for Research in Inorganic Materials, Tsukuba 305, Japan*

(Received 7 February 2000)

A novel density modification method is applied for the first time to phase reconstruction of x-ray single crystal data of quasicrystals. The structure of icosahedral Zn-Mg-Ho quasicrystals has been determined by means of this *ab initio* structure determination within a framework of a 6D description. The location, size, and shape of the occupation domains are deduced. The suggested Ho sites in the 3D structure are consistent with the results of magnetic diffuse scattering [T.J. Sato *et al.*, Phys. Rev. Lett. **81**, 2364 (1998)].

DOI: 10.1103/PhysRevLett.86.236

PACS numbers: 61.44.Br, 61.10.-i, 61.18.-j

Recently, a new group of stable icosahedral quasicrystals (*i*-QCs) [1], classified as the face-centered Frank-Kasper type, was found in the Zn-Mg-*R* (*R* = Gd, Tb, Dy, Ho or Er, and Y) system [2]. These QCs are unique, since 4*f*-electron magnetic moments are localized on the rare earth sites. The **Q** dependence of (anisotropic) magnetic diffuse scattering, observed in the *i*-ZnMgR [3,4], reflects short-range correlations of the spin system in the quasiperiodic structure. Hence, the structure as well as magnetic properties of this quasicrystal has attracted considerable interest [5]. Structural studies of *i*-ZnMgR suggest a completely different structure from previously known *i*-QCs [6,7]. However, the detailed structure is still unknown. In addition, there is no available approximant crystal for *i*-ZnMgR to guess its local structure.

The quasicrystal structure is simply represented by a 3D section of an appropriate *n*D (*n* ≥ 4) crystal (the section method) [8–10]. Within this widely accepted framework, the *i*-QC structure is described as a 6D crystal with occupation domains (ODs) extended to the 3D internal space [10]. Therefore, once a 6D structure is determined, atomic arrangement of *i*-QC in 3D external space is specified. Although a set of 6D indexed reflections is obtained from diffraction experiments, it is not an easy task to determine the 6D structure, because the so-called “phase problem” must be solved [11]. There is no direct method for QCs which allows a routine structure determination in conventional 3D crystals [11], although its generalization to 6D was discussed based on Sayre’s equation [12]. So far, several attempts to solve the problem for QCs have been mainly focused onto the use of the Patterson function [13], together in some case with contrast variation [14] and the internal space dependence of the structure factors [15,16]. When the structure of approximant crystal that has similar composition as QC is known, the phase of structure factors in QC can be deduced as demonstrated in *i*-AlCuLi [17]. The maximum-entropy method (MEM) has also been applied to QC structure analysis [18]. How-

ever, since the MEM itself needs an initial model to phase the structure factors, it was utilized as a kind of refinement method rather than a phase reconstruction method.

In this Letter, we report on the direct structure determination of *i*-Zn₆₀Mg₃₁Ho₉, by applying the low density elimination (LDE) method [19], which is an *ab initio* structure determination method based on a density modification approach in the real space. Recently, a similar approach, but based on a different principle, to solve the phase problem has been proposed [20]. However, this is the first attempt to solve the phase problem of unknown real QC structure. The location, size, and shape of the ODs in the 6D unit cell are obtained without any model structure. Moreover, the determined structure clarifies the Ho sites in the 3D structure for the benefit of its large atomic number (*Z* = 67).

A single crystal sample of *i*-Zn₆₀Mg₃₁Ho₉ was taken from well characterized large single grain obtained by the Bridgman method [21]. The sample was polished into a sphere with a diameter of 238 μm. Intensity data were collected on a conventional four-circle diffractometer with graphite-monochromatized MoKα radiation ($\lambda = 0.7107 \text{ \AA}$) from an x-ray tube. The lattice constant of a face-centered 6D cubic lattice was determined as $a_{6D} = 14.623 \text{ \AA}$ from selected 25 reflections, which corresponds to icosahedral lattice parameter $a = a_{6D}/\sqrt{2} = 10.340 \text{ \AA}$ in the external space. The reflections were corrected appropriately for Lorentz, polarization, and absorption factors. The number of 1184 reflections in total was observed from which 326 independent reflections [$F_o > 3\sigma(F_o)$, $Q_{\parallel} \leq 8.90 \text{ \AA}^{-1}$, and $Q_{\perp} \leq 1.57 \text{ \AA}^{-1}$ in units of $2\pi/a$] were obtained, where the subscripts \parallel and \perp represent its external and internal space components, respectively.

Shown in Fig. 1 is the 6D Patterson function (PF) of *i*-Zn₆₀Mg₃₁Ho₉ which represents a rather complicated structure; a feature like modulated strings is observed along the \mathbf{r}_{\perp} direction. (Hereafter, a primitive cell is employed for structural description. Therefore, even- and odd-parity

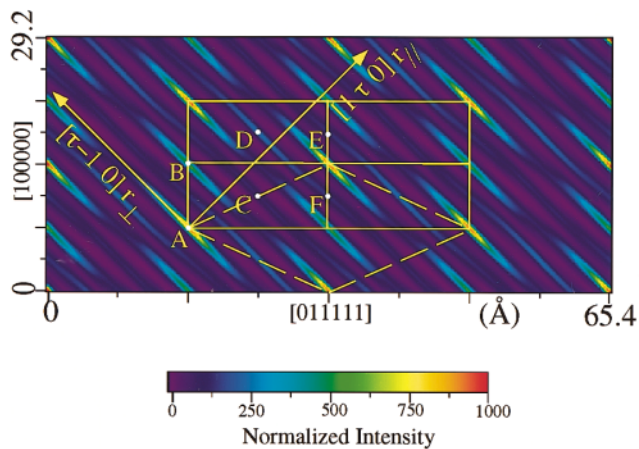


FIG. 1 (color). The rational cut of the 6D Patterson function in a plane containing a fivefold axis in both external (\mathbf{r}_{\parallel}) and internal (\mathbf{r}_{\perp}) spaces. A–F denote positions of e.V, o.V, e.B, o.B, e.E, and o.E. The outermost rectangle shows a face-centered 6D unit cell. Dashed lines represent a primitive unit cell.

cells are not equivalent to each other, while fractional coordinates are taken with the original face-centered cell.) Correlations are seen at even and odd vertices (labeled, respectively, as e.V:[000000] and o.V:[100000]/2), body centers (e.B:[111111]/4 and o.B:[311111]/4), and edge centers (e.E:[322222]/4 and o.E:[122222]/4). This strongly suggests that large ODs are located at all the sites. However, direct interpretation of the PF seems to be difficult. Our primary motivation of the present study is thus to overcome such difficulties. It is interesting to compare this PF with that of, e.g., *i*-AlPdMn, which has three large independent ODs (located at e.V, o.V, and o.B in our notation) in the 6D unit cell [16]. This simple 6D structure shows well separated blobs of high intensity region even in the PF. In such a case, the Patterson analysis is effective; then by assuming the position and size of ODs, it can be a starting point for further analysis.

The phase reconstruction by the direct methods is done exclusively in the reciprocal space by applying mathematical relationships between phases, which is based on the properties of electron density in a crystal structure: *atomicity* and *positivity* [11]. The LDE method performs calculation so as to comply with these conditions in the real space [19]. This approach has been extended to cover nD crystals and then tested and validated for its effectiveness with several quasicrystals in both calculated and observed data sets [22,23]. The QC structure as nD crystal is rather simple, since it consists of discrete ODs. This can be considered as *atomicity* in the nD space. In the LDE method, initial electron density is calculated from a set of structure factors with completely random phases; then the density is modified repeatedly by a function

$$\rho'(\mathbf{r}) = \rho(\mathbf{r}) \left\{ 1 - \exp \left[-\frac{1}{2} \left(\frac{\rho(\mathbf{r})}{0.2\rho_c} \right)^2 \right] \right\} \quad \rho(\mathbf{r}) \geq 0,$$

$$\rho'(\mathbf{r}) = 0 \quad \rho(\mathbf{r}) < 0,$$

where $\rho(\mathbf{r})$ and $\rho'(\mathbf{r})$ represent prior and modified density at position \mathbf{r} and ρ_c is an average density in the nD unit cell. This function removes negative density and sharpens peaks and the procedure is continued until the average change of phases becomes less than a predetermined limit (normal value is 0.5°). It should differentiate between the LDE method and the similar method recently proposed by Elser [20]. The latter changes phases directly so as to accomplish small global minimum densities in the unit cell, where the densities are evaluated at randomly chosen positions. In the LDE method, the structure solution is obtained as a result of multisolution calculation. The number of trials to get the solution is comparatively small. The solution can easily be found in the results and confirmed by further analysis. The reconstructed phase set by the LDE method always contains wrongly assigned phases which make the resultant density distribution somewhat obscure. However, it is not the problem to deduce location, size, and shape of the ODs. For a centrosymmetric model of *i*-AlPdMn [24], 472 out of 659 reflections (it includes all strong reflections having $Q_{\perp} > 0.4 \text{ \AA}^{-1}$ and amplitude ratio $F_o/F_{o,\max} > 0.06$) were assigned correctly [22,23].

Structure determination of *i*-ZnMgHo has been performed by applying the 6D LDE method with $(14)^6$ grid points using 238 independent reflections ($Q_{\parallel} \leq 8.90 \text{ \AA}^{-1}$ and $Q_{\perp} \leq 1.50 \text{ \AA}^{-1}$). An optimized fast Fourier transform routine was utilized for the 6D Fourier transform [25]. Only the center of symmetry was assumed and 28 resultant densities were identical out of 100 trials. We are convinced that these densities are the solutions by subsequent analysis. Figure 2 shows the 2D cut of the 6D density calculated with the reconstruct phases. We see blobs of the high density region, which represents a section of OD, at all the sites (A–F) indicated in the figure. The largest and densest OD is situated at o.B, which is quite different from that located at e.B. This structure is different from that of *i*-Zn₅₀Mg₄₂Y₈ reported previously [6].

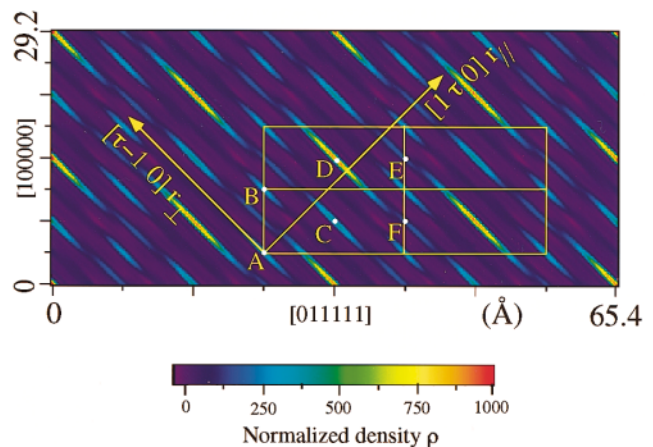


FIG. 2 (color). The rational cut of 6D density [not including $F(000000)$] calculated with reconstructed phases in a plane containing a fivefold axis in both external (\mathbf{r}_{\parallel}) and internal (\mathbf{r}_{\perp}) spaces. The meaning of A–F is the same as those described in Fig. 1.

Moreover, it should be noticed that the center of the ODs at e.E and o.E are shifted from ideal edge-center positions along the \mathbf{r}_\perp direction. The existence of such ODs was not expected in the previous study and not treated in the course of the structure analysis of $i\text{-Zn}_{47}\text{Mg}_{45}\text{Ho}_8$, appropriately [7]. The ODs at e.E and o.E are related by an inversion operation. Therefore, the structure of $i\text{-ZnMgHo}$ is characterized by the five independent ODs in the face-centered 6D unit cell, in contrast to $i\text{-AlPdMn}$, where three ODs are independent.

Figure 3 shows the cross sections of the ODs taken along the plane perpendicular to a twofold axis in the \mathbf{r}_\perp space. The ODs at e.V and o.V have approximately the same size [Figs. 3(a) and 3(b)], although a more steep profile is recognized for the latter compared with the former. An elongated shape along fivefold axes can be seen for the OD at e.B [Fig. 3(c)]. Note that these three ODs show almost the same peak height. Again we see large and dense OD at o.B [Fig. 3(d)]. Its peak height is roughly twice as high as those observed in the ODs at e.V, o.V, and e.B. This strongly suggests that Ho atoms concentrate on the OD at o.B, which is consistent with previous study [7]. The OD at e.E does not show significant symmetry in this cross section, because the center of this OD is not located on the edge-center position as mentioned above.

The ODs at edge-center positions are quite unique. It can be considered that these ODs belong to either e.B or o.B. Since the OD at o.B is large enough, we consider that these ODs belong to the e.B. As a result, one obtains a large OD at e.B, whose size is comparable with that of o.B. In this case, one should take into account a positional shift of $\sqrt{(18 - 11\tau)/(2 + \tau)}(a/2) \approx 0.61 \text{ \AA}$ (τ for golden mean) of the outward ODs at e.B along the \mathbf{r}_\parallel space. Twelve equivalent ODs (from edge center position) surround the e.B position. They are located at positions along fivefold axes. Thus, the electron density elongated along the fivefold axis in Fig. 3(c) seems to be related with those ODs. The large ODs at body center positions have been inferred previously [7]. In the previous model, unphysically short interatomic distance ($\sim 0.61 \text{ \AA}$) remains in the \mathbf{r}_\parallel space. Such a short distance universally appears, if an overlap exists when the ODs located at edge centers and body centers are projected onto the \mathbf{r}_\perp space. The determined structure in the present study shows almost no overlap between those ODs as seen in Fig. 2, suggesting the correct location of the ODs at edge-center positions. Therefore, modeling with this knowledge would avoid such unreasonably short interatomic distance in the \mathbf{r}_\parallel space.

In order to understand the \mathbf{Q} dependence of magnetic-diffuse scattering in $i\text{-ZnMgHo}$ [4], interatomic distances between Ho atoms and their directions in the \mathbf{r}_\parallel space are important. As seen in Fig. 3, it is considered that most of Ho concentrates on the OD at o.B, since Ho is the heaviest element in this structure, whose atomic number is 2 times and 5 times as large as those of Zn and Mg, respectively (see Fig. 4). However, the size of the OD seems obviously too large to expect that the OD is occupied by

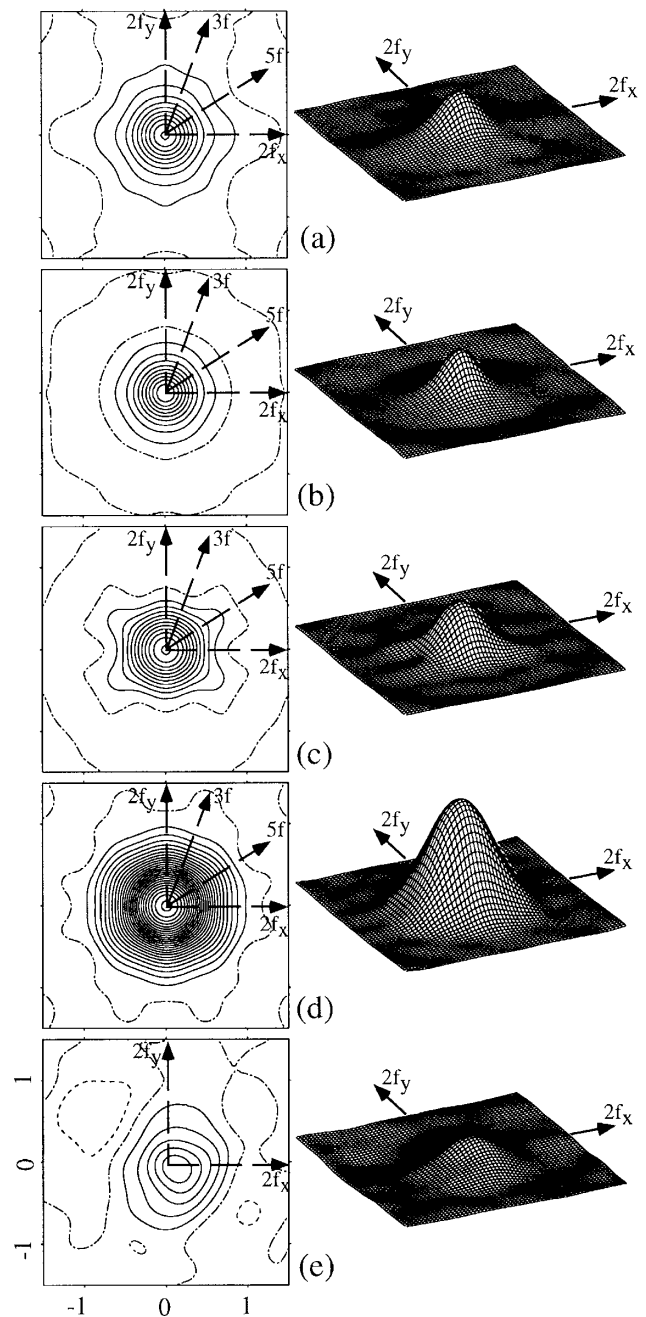


FIG. 3. Section of the ODs in the internal (\mathbf{r}_\perp) space (unit is taken by the lattice constant a). (a)–(e) correspond to the ODs at e.V, o.V, e.B, o.B, and e.E. Note that the OD at o.E is obtained by applying the inversion operation to that of e.E.

only Ho. On the other hand, if the Ho occupy the outside of the OD, a dent is probably observed at the center. Since any trace of it is not seen in Fig. 3(d), we note that the Ho occupies the center of the OD at o.B. By taking a 3D section of the determined 6D structure under the above consideration, the Ho sites can be specified in the \mathbf{r}_\parallel space. The radius of the OD is expected to be smaller than $\sqrt{(2 + 3\tau)/(2 + \tau)}a \approx 7.12 \text{ \AA}$, by considering the chemical composition of $i\text{-ZnMgHo}$. Hence, we obtain 5.44, 7.69, and 8.80 \AA as first to third nearest-neighbor

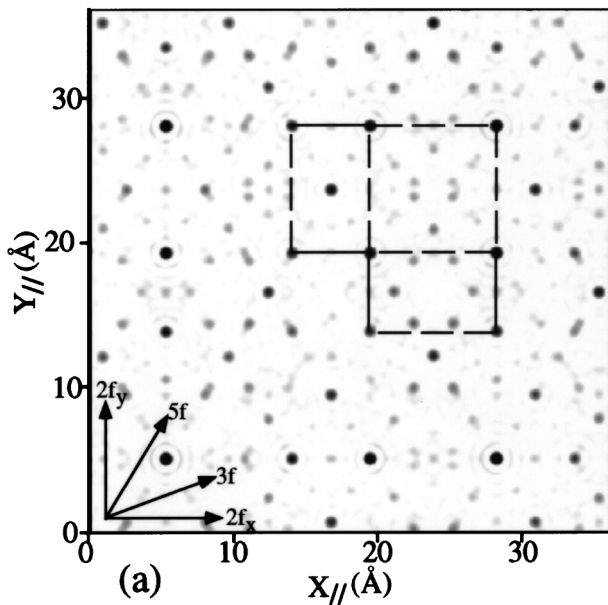


FIG. 4. A 2D cut of the 3D electron density of *i*-ZnMgHo in the external (r_{\parallel}) space perpendicular to a twofold axis. The solid and broken lines represent two dominant short Ho-Ho distances (5.44 and 8.80 Å) and the network of Ho atoms comes from OD located at o.B.

(NN) distances between Ho atoms. They correspond to the r_{\parallel} component of 6D lattice vectors, e.g., $(0, 0, 0, 1, 0, 1)/2$, $(-1, 0, 1, 0, -1, 1)/2$, and $(0, 0, 1, 0, 0, -1)/2$. The first and third distances are dominant in the structure. Indeed, strong antiferromagnetic correlation was observed for Er and Ho compounds with these correlation lengths [3,4]. Moreover, their direction in the r_{\parallel} space explains observed anisotropy of correlations well, if antiferromagnetic correlation is assumed for those Ho atoms [4,26]. The second NN distance is minor since this distance appears less frequently compared with the first and third NN distances, and is dependent on the limit radius of the OD.

The detailed shape of ODs and distribution of atomic species in them should be specified by a model fitting, e.g., polyhedral OD modeling [10], but it is not the subject of the current study. However, it should be mentioned here that a crude model fitting with ODs approximated by spherical shells gave a consistency with the above results, which gave a weighted R factor of 0.16 for all independent reflections. Further study about the construction of model structure and refinement of it is actually now in progress and will be published in a forthcoming paper.

The authors thank Akira Sato for technical support on the x-ray diffraction experiment. The numerical calculation was performed on the SX-4/20 at NRIM.

*To whom correspondence should be addressed.

- [1] D. Shechtman, I. Blech, D. Gratias, and J. W. Cahn, *Phys. Rev. Lett.* **53**, 1951 (1984).
- [2] Z. Luo, S. Zhang, Y. Tang, and D. Zhao, *Scr. Metall. Mater.* **28**, 1513 (1993); A. Niikura, A. P. Tsai, A. Inoue, and T. Masumoto, *Philos. Mag. Lett.* **69**, 351 (1994); A. P. Tsai *et al.*, *Philos. Mag. Lett.* **70**, 169 (1994).
- [3] B. Charrier, B. Ouladdiaf, and D. Schmitt, *Phys. Rev. Lett.* **78**, 4637 (1997).
- [4] T. J. Sato, H. Takakura, A. P. Tsai, and K. Shibata, *Phys. Rev. Lett.* **81**, 2364 (1998).
- [5] Y. Hattori *et al.*, *J. Phys. Condens. Matter* **7**, 2313 (1995); I. R. Fisher *et al.*, *Phys. Rev. B* **59**, 308 (1999).
- [6] A. Yamamoto *et al.*, *Philos. Mag. Lett.* **73**, 247 (1996).
- [7] T. Ohno and T. Ishimasa, in *Proceedings of the 6th International Conference on Quasicrystals*, edited by S. Takeuchi and T. Fujiwara (World Scientific, Singapore, 1998), p. 39.
- [8] M. Duneau and A. Katz, *Phys. Rev. Lett.* **54**, 2688 (1985).
- [9] T. Janssen, *Acta Crystallogr. Sect. A* **42**, 261 (1986).
- [10] For a review on structure analysis of quasicrystals, see A. Yamamoto, *Acta Crystallogr. Sect. A* **52**, 509 (1996).
- [11] See, for example, H. A. Hauptman, *Rep. Prog. Phys.* **54**, 1427 (1991).
- [12] Z. Q. Fu, F. H. Li, and H. F. Fan, *Z. Kristallogr.* **206**, 57 (1993).
- [13] D. Gratias, J. W. Cahn, and B. Mozer, *Phys. Rev. B* **38**, 1643 (1988).
- [14] C. Janot *et al.*, *Phys. Rev. Lett.* **62**, 450 (1989).
- [15] M. Cornier-Quiquandon *et al.*, *Phys. Rev. B* **44**, 2071 (1991).
- [16] M. Boudard *et al.*, *J. Phys. Condens. Matter* **4**, 10 149 (1992).
- [17] S.-Y. Qiu and M. V. Jarić, in *Quasicrystals*, edited by M. V. Jarić and S. Lundqvist (World Scientific, Singapore, 1990), p. 19.
- [18] W. Steurer *et al.*, *Acta Crystallogr. Sect. B* **49**, 661 (1993).
- [19] M. Shiono and M. M. Woolfson, *Acta Crystallogr. Sect. A* **48**, 451 (1992).
- [20] V. Elser, *Acta Crystallogr. Sect. A* **55**, 489 (1999).
- [21] T. J. Sato, H. Takakura, and A. P. Tsai, *Jpn. J. Appl. Phys., Part 2* **37**, L663 (1998).
- [22] M. Shiono, H. Takakura, and A. Yamamoto, in *Proceedings of Aperiodic 2000*, Nijmegen [Ferroelectrics (to be published)].
- [23] H. Takakura *et al.* (to be published).
- [24] A. Yamamoto *et al.*, *Mater. Sci. Forum* **150-151**, 211 (1994).
- [25] H. Watabe, M. Minami, and A. Yamamoto, Japan Atomic Energy Research Institute Report No. JAERI-Data/Code 97-038, 1997 (in Japanese).
- [26] T. J. Sato *et al.* (unpublished).